Spatial variation of T2 in human articular cartilage

Article *in* Radiology · December 1997

DOI: 10.1148/radiology.205.2.9356643 · Source: PubMed

5 authors, including:

Bernard Dardzinski
National Institutes of Health
160 PUBLICATIONS **7,652** CITATIONS
SEE PROFILE

Timothy J Mosher
Pennsylvania State University
117 PUBLICATIONS **5,932** CITATIONS
SEE PROFILE

Sirui li
Jilin University
116 PUBLICATIONS **8,950** CITATIONS
SEE PROFILE

Bernard J. Dardzinski, PhD • Timothy J. Mosher, MD • Shizhe Li, PhD
Mark A. Van Slyke, MD • Michael B. Smith, PhD

Spatial Variation of T2 in Human Articular Cartilage

PURPOSE: **To determine the spatial variation of in vivo cartilage T2 in young asymptomatic adults.**

MATERIALS AND METHODS: **Quantitative T2 maps of seven asymptomatic young male adults and one male volunteer with a history of previous intraarticular chondroid fragments were calculated by using a multiecho, spin-echo magnetic resonance imaging sequence at 3.0 T. The T2 maps were bilinearly interpolated to generate T2 profiles across the thickness of cartilage.**

RESULTS: **All seven asymptomatic volunteers demonstrated a monotonic increase in T2, which increased from 32 msec ± 1 in the deep radial zone and 48 msec ± 1 in the deep transitional zone to 67 msec ± 2 in the outer transitional superficial zone. The T2 profile of the volunteer with superficial fibrillation observed at arthroscopy demonstrated marked spatial heterogeneity and a statistically significant increase in cartilage T2.**

CONCLUSION: **There is a reproducible pattern of increasing T2 that is proportional to the known spatial variation in cartilage water and is inversely proportional to the distribution of proteoglycans. The authors postulate that these regional T2 differences are secondary to the restricted mobility of cartilage water within an anisotropic solid matrix.**

An important component of osteoarthritis is the degeneration and loss of articular cartilage. Ongoing research to characterize the process of cartilage degeneration and evaluate the effectiveness of chondroprotective agents for preserving and repairing damaged cartilage requires noninvasive techniques to identify early, reversible degeneration. Most previous magnetic resonance (MR) imaging studies have focused on techniques for assessing the morphology of articular cartilage to accurately measure the thickness and volume of cartilage (1,2). The results of early studies on isolated cartilage samples suggest an ability of MR imaging to depict changes in cartilage structure that precede cartilage loss (3,4). The ability of MR imaging and MR spectroscopy to enable noninvasive investigation of the macromolecular environment of cartilage water provides unique information that can potentially lead to a better understanding of cartilage degeneration.

Two previous studies with use of MR microscopy of isolated cartilage plugs demonstrate a spatial dependence of T2 in articular cartilage, with values increasing from the subchondral bone towards the articular surface (5,6). This pattern is proportional to the known distribution of water content in cartilage and is inversely proportional to the distribution of proteoglycans (7). Because tissue T2 is dependent on the slow molecular motion of water, we assumed that these regional differences reflect inherent differences in water mobility secondary to the surrounding macromolecular matrix. It is likely that early degenerative change in the cartilage matrix will alter the mobility, and thus the T2, of cartilage water. Thus far, to our knowledge, these techniques have not been applied in vivo. In this study, we evaluated the spatial variation of T2 in the patellar cartilage of young asymptomatic volunteers.

MATERIALS AND METHODS

MR Imaging

From January 1996 to July 1996, we evaluated the right knee of seven asymptomatic male volunteers (mean age, 34 years; age range, 24–40 years) and of one male volunteer (aged 35 years) who demonstrated superficial fibrillation at arthroscopy. Informed written consent was obtained from all volunteers after the nature of the procedure had been fully explained.

MR imaging experiments were performed on a Medspec S300 3.0-T imaging-spectrometer (Bruker Instruments, Karlsruhe, Germany) operating at 125 MHz for protons (hydrogen-1). A 33-cm-diameter asymmetric gradient insert, capable of delivering ±6 G/cm, was used in all imaging experiments. B_1 field generation and signal reception was accomplished with a 9-cm transmit-receive surface coil. Data were acquired in the axial plane through the middle of the patella prescribed from a sagittal locator image. Proton-density and

Index terms: Cartilage, MR, 4521.121411 • Magnetic resonance (MR), high-field-strength imaging, 4521.121411, 4521.12146 • Magnetic resonance (MR), relaxometry, 4521.12146 • Magnetic resonance (MR), tissue characterization, 4521.12146

Radiology 1997; 205:546–550

[1] From the Departments of Radiology, Center for NMR Research (B.J.D., T.J.M., S.L., M.A.V.S., M.B.S.), and Cellular and Molecular Physiology (M.B.S.), Pennsylvania State University College of Medicine, Milton S. Hershey Medical Center, 500 University Dr, Hershey, PA 17033. From the 1996 RSNA scientific assembly. Received May 8, 1997; revision requested June 19; revision received July 9; accepted July 10. **Address reprint requests to** T.J.M.

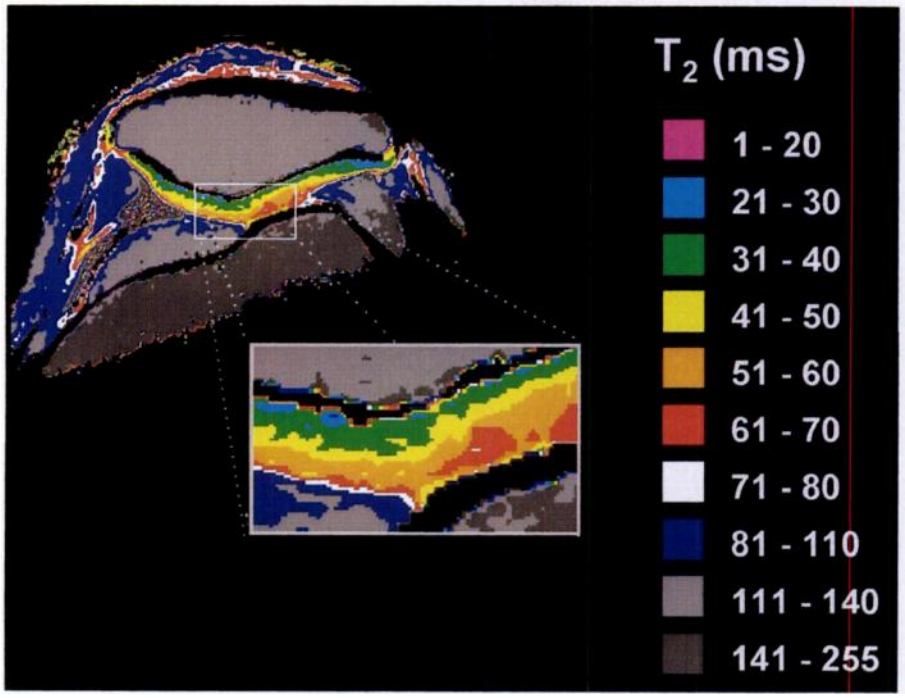

Figure 1. Color map of T2 in patellar cartilage from an asymptomatic young adult demonstrates a progressive increase in the T2 from the radial to the superficial zone.

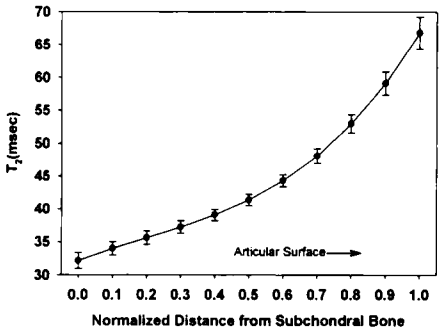

Figure 2. Mean T2 (± standard error of the mean) versus normalized distance from subchondral bone for seven asymptomatic young male volunteers demonstrates a smooth monotonic increase in T2 from the deep radial zone to the superficial zone. Values are averaged from the middle of the medial and lateral facets and the median ridge.

T2 maps were calculated from 11 axial spin-echo images simultaneously acquired through the middle of the patella with a multiecho spin-echo imaging sequence. Imaging parameters were as follows: repetition time of 1,500 msec, echo time from 9 to 99 msec in 9-msec increments, 3-mm section thickness, 8-cm field of view, 128 × 128 matrix, 50-kHz bandwidth, section-selection and refocusing pulse widths of 2,000 msec, two signals acquired, total acquisition time of 6.5 minutes. The read-encoding (frequency) axis was chosen in the left-to-right direction, across the patella, to minimize chemical shift artifact at the patellar cartilage-bone interface. Cartilage thickness was calculated from axial gradient-echo images with the following parameters: 200/13 (repetition time msec/echo time msec), 45° flip angle, 3-mm section thickness, 8-cm field of view, 256 × 256 matrix, 25-kHz bandwidth, section-selection pulse width of 4,000 msec, four signals acquired, total acquisition time of 3.5 minutes.

Data Analysis

Proton-density and T2 maps were calculated from the 11 spin-echo images by using nonlinear least squares curve fitting, on a pixel-by-pixel basis, with Interactive Data Language (IDL Research Systems, Boulder, Colo). Fitting the signal intensity, SI, for the i^{th}, j^{th} pixel as a function of time, t, can be expressed as follows: $SI_{i,j}(t) = S0_{i,j} \cdot \exp(-t/T2_{i,j})$, where $S0_{i,j}$ is the pixel intensity at $t = 0$, and $T2_{i,j}$ is the T2 time constant of pixel i, j. A proton-density map is generated from the pixel $S0_{i,j}$ data, and a T2 map (image) is generated from the $T2_{i,j}$ data. The T2 map was then bilinear interpolated to a 512 × 512 image matrix. T2 profiles were acquired through the median ridge and the middle of the medial and lateral facets of the patellar cartilage. Each profile was normalized for distance and fit with a cubic polynomial for comparison between volunteers. The mean and standard deviation of T2 was then plotted as a function of normalized distance for the seven asymptomatic volunteers. The T2 maps were color coded to represent a specific range of values. With the gradient-echo images, cartilage thickness was measured perpendicular to the bone-cartilage interface of the middle of the medial and lateral facets and the median ridge.

RESULTS

Figure 1 depicts the color-coded T2 map of an axial section through the patellar cartilage from a representative asymptomatic volunteer. T2 values range from 30 to 70 msec within the cartilage and greater than 100 msec in the patellar marrow space. The laminar appearance of T2 values within the cartilage is a function of the color coding used for illustration. T2 values as a function of normalized distance from the subchondral bone are illustrated in Figure 2. Each point in this graph represents the mean ± standard error of the mean of the three profiles for seven asymptomatic volunteers for all three locations. All volunteers demonstrated a monotonic increase in T2, increasing from 32 msec ± 1 in the deep radial zone and 48 msec ± 1 in the deep transitional zone to 67 msec ± 2 in the outer transitional zone ($P < .001$). Due to the spatial resolution of the T2 measurement, the histologic superficial zone was not resolved. For the symptomatic volunteer, the monotonic increase in T2 was not observed. In the median ridge, the T2 measured 51 msec in the deep radial zone, 56 msec in the deep transitional zone, and 41 msec in the outer transitional zone. Mean cartilage thickness (± standard error of the mean) measured on gradient-echo images of the seven asymptomatic volunteers was 4.2 mm ± 0.4, 4.1 mm ± 0.4, and 4.2 mm ± 0.3 for the medial facet, median ridge, and lateral facet, respectively.

DISCUSSION

Current theories on the biomechanical properties of articular cartilage stress the importance of fluid transport and cartilage permeability in determining the response to compressive stress (8). The viscoelastic behavior of cartilage, which is determined by the mobility of cartilage water, has been previously studied with use of destructive techniques. Biophysical techniques such as compression creep experiments provide information on the material properties of excised cartilage tissue, and characterize the bulk properties of fluid flux (9). The measurement of streaming potentials, which are generated by ionic fluid flux through cartilage with compression, has poor spatial resolution and is limited to excised samples (10,11). Combined histologic-compression techniques have been described to evaluate regional strain (12,13) and thus can indirectly characterize the movement of cartilage fluid. The information obtained noninvasively through MR imaging and MR spectroscopy is unique in its ability to facilitate characterization of the macro-

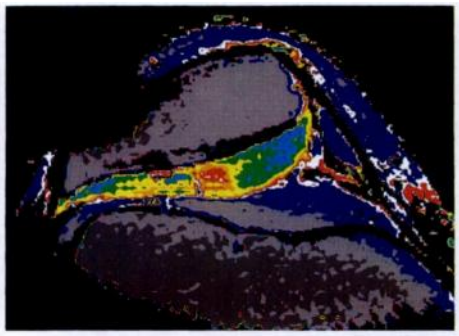

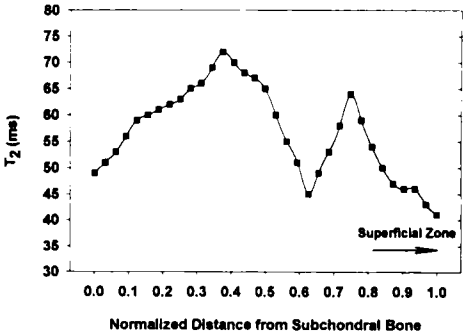

3. 4a. 4b.

Figures 3, 4. **(3)** Gradient-echo MR image (150/21, 45° flip angle) in a symptomatic 35-year-old man and the corresponding arthroscopic images (insets). The lateral facet contains heterogeneous internal signal intensity, with irregularity of the surface. Arthroscopic visualization (right inset) confirms moderate fibrillation and superficial erosion. The medial facet has an indistinct hyperintense superficial zone. At arthroscopy (left inset), there was evidence of mild fibrillation. **(4a)** T2 map of the patellofemoral joint shown in **3**. In the lateral facet, there is an overall increase in the T2 values and loss of the normal laminar appearance. The medial facet, which demonstrated superficial fibrillation at arthroscopy, shows uncharacteristically low T2 values in the deep and radial zones. **(4b)** T2 profile across the median ridge demonstrates the increased T2 values in the deep and transitional zones.

molecular environment of water protons and probe the important interaction of cartilage fluid with the solid matrix. As MR imaging is nondestructive, it is the only technique available to monitor long-term temporal changes in cartilage water mobility.

The results of several previous studies indicate that regional differences in the solid matrix affect the relaxation properties of cartilage water. Initial studies by Lehner et al (14) and later studies by Modl et al (15) and Rubenstein et al (16) demonstrate zonal differences in signal intensity that are postulated to be secondary to regional differences in collagen and proteoglycan concentrations identified at histologic examination. Paul and co-workers (17) suggest that the variation in signal intensity of human patellar cartilage is secondary to zonal variation in proteoglycan concentration but does not correlate with the known distribution of collagen or free water concentration.

T2 of Normal Articular Cartilage

In this study, the observed spatial dependence of T2 is in excellent agreement with two previous studies obtained at high magnetic field strength (7 T). With use of H-1 MR microscopy of excised canine articular cartilage plugs, Xia and colleagues (5) demonstrated a relatively uniform distribution of T1 values; however, the T2 values are nonuniform, with the T2 increasing from 10 msec at the subchondral bone layer to 50 msec at the articular surface. They postulate that the spatial variation in T2 is secondary to the known distribution of proteoglycan concentration. A similar pattern recently has been described in excised cartilage plugs from human femoral head samples (6). The pattern of increasing T2 from the deep radial zone to the articular surface closely resembles the known spatial variation of water content in articular cartilage (18,19). We postulate that these regional differences in cartilage T2 are secondary to the restricted mobility of cartilage water within an anisotropic solid matrix.

Tissue T2 is sensitive to the slow molecular motions of the water protons and the macromolecular environment. In cartilage, the highly structured architecture of the collagen framework results in anisotropy of the dipole-dipole interactions. The large biopolymers reduce the rotational and translational motion of water protons. Because of the restricted mobility, the dipole-dipole interactions are not averaged. This produces an efficient mechanism for spin-spin relaxation (20), which reduces the T2 of cartilage water.

Several factors can limit the accuracy and precision of the T2 measurements. There is a radio-frequency flip angle dependence for surface coils as a function of depth perpendicular to the plane of the surface coil. Due to the geometry of the patellofemoral joint, the patellar cartilage is positioned in the isocenter of the surface coil where there is maximal B_1 homogeneity (21). At the beginning of each study, the 90° and 180° section-selective pulses are optimized by maximizing the signal intensity. The maximum signal intensity originates from the cartilage providing confidence that the flip angles were set properly for accurate T2 quantification. Imperfection in the 180° refocusing pulse gives rise to the formation of stimulated echoes with accumulation of magnetization along the z axis. As this component decays as a function of T1 rather than T2 decay, this will lead to an overestimation of the T2 value (22). To minimize the formation of stimulated echoes, spoiler gradients were used to disperse the unfocused magnetization. Off-resonance effects were minimized by acquiring the data as a single section. Previous reported values of cartilage T2 range from 24 to 77 msec, with longer values observed in the more superficial layers (14,23–26). Given the excellent agreement of our measured T2 with that of previous studies, in which T2 was measured with both MR spectroscopic and MR imaging techniques, the error due to T1 contamination is believed to be small. As there is little variation in T1 across the layers of articular cartilage (5,27), the effect of T1 contamination should have a negligible effect on the observed spatial variation in T2.

Pixel resolution was chosen as 625 μm in-plane (80 mm/128 pixels) with a 3-mm section thickness (1.2-μL voxels) to limit the total acquisition time of the experiment to 6.5 minutes and to provide an adequate signal-to-noise ratio. A bandwidth of 50 kHz was chosen to ensure adequate signal-to-noise ratio in the 11 spin-echo images while minimizing the interecho delay to 9 msec. This short delay is necessary to accurately fit the data for regions of relatively short T2 ($T2 < 30$ msec). For several volunteers, T2 maps were acquired with a 256×256 matrix. Although the measured T2 values and spatial dependency were equivalent to the reported measurements obtained with a 128×128 matrix, the lower signal-to-noise ratio and increased interecho time produced greater uncertainty in the calculated T2 value. For quantification,

the calculated T2 maps were interpolated to a 512 × 512 matrix to increase the average number of pixels in the profile across the patellar cartilage to 26. Interpolating and fitting the profile with a cubic polynomial smooths the monotonically increasing T2 profiles across the patellar cartilage.

For calculation of T2, data were fit to a single exponential. We recently used a multiecho, spin-echo MR spectroscopy technique to demonstrate the multiexponential T2 decay of cartilage water (28). A second, tightly bound compartment of water with a mean T2 of 250 μsec is observed. Given the short T2, this population of water protons does not contribute to the calculated T2 values reported in this study. For measurements made within a small voxel, there is little volume averaging, and a single exponential fit agrees best with the observed data. Evaluating the decaying signal intensity with a two or three exponential fit requires more images with echo times substantially less than 1 msec.

Although this study does not address the orientation dependence of T2 in cartilage, previous studies on excised samples suggest that the T2 values of the deep radial zone will be longer at sites where the surface is oriented 55° relative to the constant magnetic induction field (B_0) (6,29). Investigators attribute these findings to the "magic angle effect," which can be seen in highly structured anisotropic tissues (16,30–32). In addition, Rubenstein et al (33) recently demonstrated that the zonal appearance is dependent on the degree of compression applied to the cartilage sample and is hypothesized to result from a combination of net water loss and change in the orientation of the collagen fibers. Most of these observations were made in disarticulated samples. It is not as clear if intact living joints, which experience an intrinsic degree of compression due to the tension of ligaments and muscles, will demonstrate the same degree of orientation dependence. A quantitative evaluation of the orientation dependence of cartilage T2 in the intact living joint, to our knowledge, has not yet been reported. Results from excised samples and qualitative observations from clinical images support the theory that the spin-spin relaxation behavior of cartilage water is strongly influenced by the orientation of the collagen framework and suggest that dipole-dipole anisotropy in the presence of restricted water mobility is a major pathway for spin-spin relaxation in the deep layers of cartilage.

T2 of Damaged Articular Cartilage

Previous studies with use of excised cartilage plugs demonstrate the permeability of cartilage is increased with the onset of cartilage degeneration (34). The earliest detectable change in degeneration is an increase in water content, associated with an increase in cartilage permeability (35). As the permeability increases, hydrodynamic fluid pressure is unable to maintain load support, and greater stress is generated in the solid matrix. This stress leads to the degeneration and fragmentation of the proteoglycan-collagen matrix and a subsequent loss of cartilage tissue.

Initial observations demonstrate an increase in cartilage T2 with early degenerative change. Gradient-echo images and T2 maps were obtained for a 35-year-old volunteer with a history of prior arthroscopic surgery for free chondroid fragments. As presented in Figure 3, the gradient-echo images demonstrate heterogeneity and superficial irregularity in the lateral patellar facet; this finding corresponded to moderate fibrillation and superficial erosion at arthroscopy performed 2 days after the MR imaging examination (Fig 3, right inset). The medial facet demonstrates an indistinct superficial hyperintense zone that corresponded to mild superficial fibrillation at arthroscopy. The T2 map and T2 profile of the median ridge are presented in Figure 4. In comparison to the normal pattern of T2 spatial dependency shown in Figures 1 and 2, there is marked heterogeneity in the distribution of T2 values of the lateral facet with a substantial increase in T2 of the radial and transitional zones. This observation is compatible with an increased mobility of water protons and may also reflect the loss of normal anisotropy present in the radial zone of cartilage due to damage to the collagen-proteoglycan matrix.

In conclusion, our results demonstrate a reproducible spatial dependence of cartilage water T2. As these results were obtained from a selected population of young asymptomatic volunteers, they should not be extrapolated to older populations. Additional studies are needed to determine how normal aging changes will alter the T2 values and distribution. The results of previous studies conducted on animal models and excised human cartilage samples suggest that degenerative changes in cartilage increase water content and produce a measurable increase in cartilage T2. Our initial observations support these preliminary studies and demonstrate that these experiments can be performed in vivo. Noninvasive methods such as MR imaging provide unique information on the mobility of cartilage water and allow repeatable measurements to be made in the intact joint. This information will aid in the understanding and treatment of osteoarthritis and traumatic cartilage injury and in monitoring the maturation of cartilage transplants. ■

Acknowledgments: The authors express their gratitude to Salvatore Larusso, BS, RDMS, RTR, and Wayne Conrad, MD, for their assistance with acquisition of the arthroscopic images.

References

1. Peterfy CG, van Dijke CF, Ying L, et al. Quantification of the volume of articular cartilage in the metacarpophalangeal joints of the hand: accuracy and precision of three-dimensional MR imaging. AJR 1995; 165:371–375.
2. Sittek H, Eckstein F, Gavazzeni A, et al. Assessment of normal patellar cartilage volume and thickness using MRI: an analysis of currently available pulse sequences. Skeletal Radiol 1996; 25:55–62.
3. Bashir A, Gray ML, Burstein D. Gd-DTPA as a measure of cartilage degradation. Magn Reson Med 1996; 36:665–673.
4. Xia Y, Farquhar T, Burton-Wurster N, Vernier-Singer M, Lust G, Jelinski LW. Self-diffusion monitors degraded cartilage. Arch Biochem Biophys 1995; 323:323–328.
5. Xia Y, Farquhar T, Burton-Wurster N, Ray E, Jelinski LW. Diffusion and relaxation mapping of cartilage-bone plugs and excised disks using microscopic magnetic resonance imaging. Magn Reson Med 1994; 31:273–282.
6. Mlynarik V, Degrassi A, Toffanin R, Vittur F, Cova M, Pozzi-Mucelli RS. Investigation of laminar appearance of articular cartilage by means of magnetic resonance microscopy. Magn Reson Imaging 1996; 14: 435–442.
7. Mankin HJ, Brandt KD. Biochemistry and metabolism of articular cartilage in osteoarthritis. In: Moskowitz RW, Howell DS, Goldberg VM, Mankin HJ, eds. Osteoarthritis: diagnosis and medical/surgical management. 2nd ed. Philadelphia, Pa: Saunders, 1992; 109–154.
8. Mow VC, Holmes MH, Lai WM. Fluid transport and mechanical properties of articular cartilage: a review. J Biomechanics 1984; 17:377–394.
9. Mow VC, Zhu W, Ratcliffe A. Structure and function of articular cartilage and meniscus. In: Mow VC, Hayes WC, eds. Basic orthopedic biomechanics. New York, NY: Raven, 1991; 143–198.
10. Kim YJ, Bonassar LJ, Grodzinsky AJ. The role of cartilage streaming potential, fluid flow and pressure in the stimulation of chondrocyte biosynthesis during dynamic compression. J Biomech 1995; 9:1055–1066.
11. Garon M, Guardo R, Savard P, Buschmann P. Spatially resolved detection of streaming potentials in articular cartilage (abstr). In: Transactions of the 43rd Annual Meeting of the Orthopedic Research Society. Palatine, Ill: Orthopedic Research Society, 1997; 80–14.
12. Guilak F, Ratcliffe A, Mow VC. Chondrocyte deformation and local tissue strain in articular cartilage: a confocal microscopic study. J Orthop Res 1995; 13:410–421.

13. Broom ND, Myers DB. A study of the structural response of wet hyaline cartilage to various loading situations. Conn Tissue Res 1980; 7:227–237.
14. Lehner KB, Rechl HP, Gmeinwiesser JK, Heuck AF, Lukas HP, Kohl HP. Structure, function, and degeneration of bovine hyaline cartilage: assessment with MR imaging in vitro. Radiology 1989; 170:495–499.
15. Modl JM, Sether LA, Haughton VM, Kneeland JB. Articular cartilage: correlation of histologic zones with signal intensity at MR imaging. Radiology 1991; 181:853–855.
16. Rubenstein JD, Kim JK, Morava-Protzner I, Stanchev PL, Henkelman RM. Effects of collagen orientation on MR imaging characteristics of bovine articular cartilage. Radiology 1993; 188:219–226.
17. Paul PK, Jasani MK, Sebok D, Rakhit A, Dunton AW, Douglas FL. Variation in MR signal intensity across normal human knee cartilage. Magn Reson Imaging 1993; 3:569–574.
18. Lipshitz H, Etheridge R, Glimcher MJ. Changes in hexosamine content and swelling ratio of articular cartilage as a function of depth from the surface. J Bone Joint Surg [Am] 1976; 58:1149–1153.
19. Maroudas A, Venn M. Chemical composition and swelling of normal and osteoarthritic femoral head cartilage. Ann Rheum Dis 1977; 36:399–406.
20. Packer KJ. The dynamics of water in heterogeneous systems. Phil Trans R Soc Lond B 1977; 278:59–87.
21. Styles P, Smith MB, Briggs RW, Radda GK. A concentric surface-coil probe for the production of homogeneous B1 fields. J Magn Reson 1985; 62:397–405.
22. Poon CS, Henkelman RM. Practical T_2 quantitation for clinical applications. JMRI 1992; 2:541–553.
23. Gahunia HK, Lemaire C, Babyn PS, Cross AR, Kessler MJ, Pritzker KPH. Osteoarthritis in rhesus macaque knee joint: quantitative magnetic resonance imaging tissue characterization of articular cartilage. J Rheumatol 1995; 22:1747–1756.
24. Kim DK, Ceckler TL, Hascall VC, Calabro A, Balaban RS. Analysis of water-macromolecule proton magnetization transfer in articular cartilage. Magn Reson Med 1993; 29:211–215.
25. Duewell SH, Ceckler TL, Ong K, et al. Musculoskeletal MR imaging at 4 T and 1.5 T: comparison of relaxation times and image contrast. Radiology 1995; 196:551–555.
26. Kaufman JH, Cecil KM, Kneeland JB, Bolinger L. Structure in image of articular cartilage at 4T (abstr). In: Proceedings of the Fourth Meeting of the International Society for Magnetic Resonance in Medicine. Berkeley, Calif: International Society for Magnetic Resonance in Medicine, 1996; 834.
27. Freeman DM, Bergman G, Glover G. Short TE microscopy: accurate measurement and zonal differentiation of normal hyaline cartilage. Magn Reson Med 1997; 38:72–81.
28. Mosher TJ, Dardzinski BJ, Smith MB. Characterization of multiple T_2 components in articular cartilage (abstr). In: Proceedings of the Fifth Meeting of the International Society for Magnetic Resonance in Medicine. Berkeley, Calif: International Society for Magnetic Resonance in Medicine, 1997; 1331.
29. Xia Y, Farquhar T, Burton-Wurster N, Lust G. T_2 relaxation anisotropy as a sensitive signature for the orientation of molecular networks in cartilage (abstr). In: Transactions of the 43rd Annual Meeting of the Orthopedic Research Society. Palatine, Ill: Orthopedic Research Society, 1997; 218–237.
30. Henkelman RM, Stanisz GJ, Kim JK, Bronskill MJ. Anisotropy of NMR properties of tissues. Magn Reson Med 1994; 32:592–601.
31. Dunn JF, Goodwin DW. Micro-imaging and the magic angle effect in cartilage (abstr). In: Proceedings of the Fourth Meeting of the International Society for Magnetic Resonance in Medicine. Berkeley, Calif: International Society for Magnetic Resonance in Medicine, 1996; 206.
32. Shinar H, Eliav U, Schneiderman R, Maroudas A, Navon G. ^{2}H and ^{23}Na Multiple quantum filtered NMR spectroscopy and diffusion measurements of human articular cartilage (abstr). In: Proceedings of the Third Meeting of the International Society for Magnetic Resonance in Medicine. Berkeley, Calif: International Society for Magnetic Resonance in Medicine, 1995.
33. Rubenstein JD, Kim JK, Henkelman RM. Effects of compression and recovery on bovine articular cartilage: appearance on MR images. Radiology 1996; 201:843–850.
34. Armstrong CG, Mow VC. Variations in the intrinsic mechanical properties of human articular cartilage with age, degeneration, and water content. J Bone Joint Surg [Am] 1982; 64:88–94.
35. McDevitt CA, Muir H. Biochemical changes in the cartilage of the knee in experimental and natural osteoarthritis in the dog. J Bone Joint Surg [Br] 1976; 58:94–101.